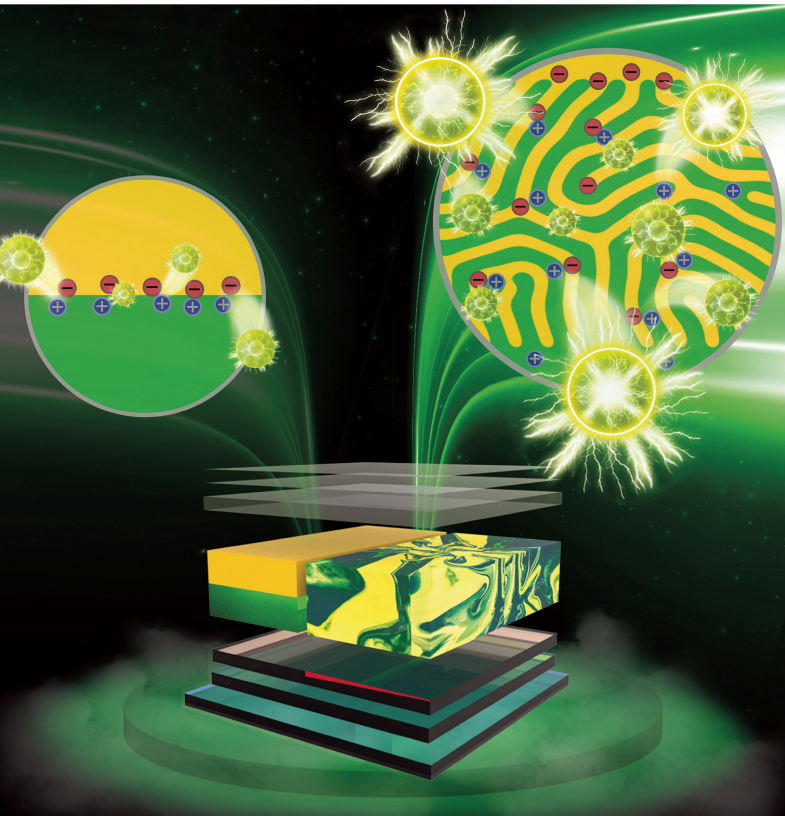


ACS APPLIED ELECTRONIC MATERIALS

April 2020
Volume 2
Number 4
pubs.acs.org/acsaem



ACS Publications
Most Trusted. Most Cited. Most Read.

www.acs.org

A Comparative Study via Photophysical and Electrical Characterizations on Interfacial and Bulk Exciplex-Forming Systems for Efficient Organic Light-Emitting Diodes

Nurul Ridho Al Amin, Kiran Kishore Kesavan, Sajal Biring, Chih-Chien Lee, Tzu-Hung Yeh, Tzu-Yu Ko, Shun-Wei Liu,* and Ken-Tsung Wong*



Cite This: *ACS Appl. Electron. Mater.* 2020, 2, 1011–1019



Read Online

ACCESS |



Metrics & More



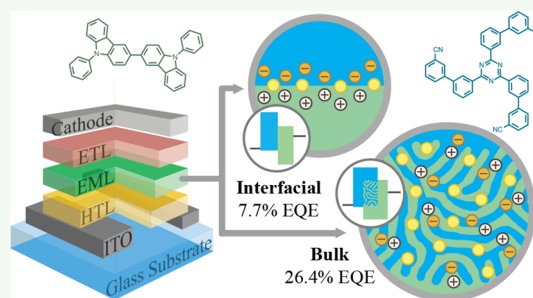
Article Recommendations



Supporting Information

ABSTRACT: An efficient organic light-emitting diode based on the BCzPh:CN-T2T exciplex as an emitting layer (EML) has been fabricated by exploiting charge balance and favorable molecular orientations. To further understand the details of the exciplex-forming mechanism, time-resolved photoluminescence (TRPL), capacitance-voltage (CV), impedance spectroscopy (IS), and transient electroluminescence (EL) measurements were used to probe the photophysical and electrical characteristics of EL devices by incorporating interfacial (BCzPh/CN-T2T) and bulk (BCzPh:CN-T2T) exciplexes as the emitting layer. Interfacial- and bulk-exciplex devices exhibit a maximum external quantum efficiency (EQE) of 7.7 and 26.4%, respectively. The reason for different device performances was rationalized by comparing the accumulated amount of charge density at the EML's interface responsible for exciplex emission. In addition, the TRPL measurement monitored from short to long wavelengths was used to explore the harvest of nonradiative triplets back to singlets via reverse intersystem crossing and to examine the efficiency of delayed fluorescence. The bulk-exciplex system showed a distinct delayed fluorescence as compared to the interfacial one, which was also corroborated by the observation in the transient EL. The result indicates that the bulk exciplex can reduce the accumulated charge in the EML rapidly, resulting in improvement of EL efficiency. This assumption was further verified by CV and IS measurements. Our results reveal that the accumulated charge density and the bulk resistance of the bulk-exciplex device are much lower as compared to those of the interfacial counterpart device.

KEYWORDS: *interfacial exciplex, bulk exciplex, transient photoluminescence, impedance spectroscopy, transient electroluminescence*



INTRODUCTION

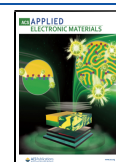
Over the past decade, organic light-emitting diodes (OLEDs) based on thermally activated delayed fluorescence (TADF) have attracted a lot of researchers' attention and have appeared as promising candidates for flat panel display and illumination applications.^{1,2} According to spin statistics, the hole and electron recombination within an organic material gives 25% of the singlet exciton, which is responsible for the fluorescence emission, whereas the emission from the rest of the 75% triplet exciton is forbidden. The TADF mechanism offers the advantage of realizing 100% internal quantum efficiency (IQE) by harvesting nonemissive triplet excitons.^{3–5} Besides the utilization of 100% excitons, TADF-based OLEDs also show extraordinary features such as high efficiency, bright luminance, lower driving voltage, lower power consumption, and low-cost organic materials.^{6–8} Theoretically, TADF can be realized by the manipulation of the subtle overlap between the highest occupied molecular orbital (HOMO) and the lowest unoccupied molecular orbital (LUMO), resulting in a small exchange energy or a small singlet–triplet energy gap (ΔE_{ST}), which is beneficial for facilitating the up-conversion of the

triplet exciton back to the singlet exciton via the reverse intersystem crossing (RISC) process. To achieve a small ΔE_{ST} , one of the promising approaches is the utilization of intramolecular charge transfer (ICT) with tailor-made molecules comprising judiciously selected donor (D) and acceptor (A) moieties that are linked into a twisted molecular configuration.^{9,10} Since 2012, Adachi et al. demonstrated the feasibility of harvesting triplet energy via the up-conversion mechanism by virtue of the RISC process using a molecule with a small ΔE_{ST} .¹¹ Many highly efficient OLEDs based on the TADF strategy have been reported.^{12,13} Particularly, the TADF-based device with a maximum external quantum efficiency (EQE) of over 38% has been recently reported.¹⁴

Received: January 24, 2020

Accepted: March 24, 2020

Published: March 24, 2020



The effective up-conversion mechanism can also be realized by forming an exciplex via intermolecular charge transfer occurring at the interface of physically blended donor and acceptor.^{15–17} Exciplex formation leads to well-separated HOMOs and LUMOs localized on the donor and the acceptor, respectively, giving a limited exchange energy and thus rendering TADF feasible. Furthermore, the exciplex that exhibits TADF behavior can achieve a smaller ΔE_{ST} by decreasing the exchange energy as the separation distance between the HOMO of the donor and the LUMO of the acceptor increases.¹⁸ There are mainly two kinds of exciplex-forming systems that have been reported, i.e., interfacial and bulk exciplex systems.^{19,20} In the interfacial exciplex system, the exciplex is formed at the interface of the pristine donor and acceptor layer, and the excitons are created along the surface of the interfacial area.²¹ In recent years, OLEDs based on the interfacial exciplex have been reported to exhibit EQEs up to 19%.²² On the other hand, an emission layer (EML) is designed in a bulk exciplex system by mixing the donor and acceptor materials, and the excitons are formed throughout the EML.²³ Recent progress in TADF-based OLEDs with the bulk exciplex as the EML has shown over 21% EQE.²⁴

Comparison of the exciplex-forming strategy between the “interfacial and bulk” approaches for exciplex-based OLEDs has been limitedly done in recent years. For example, in 2013, Hung et al. demonstrated an efficient interfacial exciplex device with a current efficiency (CE), power efficiency (PE), and EQE of 22.5 cd A⁻¹, 23.6 lm W⁻¹, and 7.7% respectively. In comparison, a bulk exciplex device with a 25 nm EML did not show much better performance rather than a slight increase in CE, PE, and EQE up to 23.6 cd A⁻¹, 26.0 lm W⁻¹, and 7.8% respectively.²⁵ But in 2014, Hung et al. showed a considerable improvement in the performance of the bulk exciplex device compared to the interfacial exciplex one.²⁶ The bulk exciplex not only offers an increase in the intermolecular contacts but also improves the device efficiency. In 2019, an efficient bulk exciplex device with EQEs up to 20% was achieved by Chapran et al. They reported the photophysical process in the bulk exciplex using photoluminescence (PL) measurements on the devices fabricated with a common acceptor that was combined with different donor molecules for providing emission from blue to red orange.²⁷ Based on these examples, we found that the lack of detailed characterizations on the device physics as well as the RISC process might impede the further development of new efficient exciplex systems. To address the energy transfer mechanism in the TADF exciplex system, our group reported the relationship between spin-orbit coupling, the energy gap of the singlet and triplet, and the polarization parameter for efficient conversion from triplet excitons to singlet excitons.²⁸

In the last 5 years, impedance spectroscopic (IS) characterization has been widely used to understand the intrinsic properties of OLEDs, such as the degradation mechanism²⁹ and dynamics of mobile charge,³⁰ as well as interfacial charge³¹ and equivalent circuit of devices.^{32,33} For example, Chapran et al.³⁴ reported in 2015 a comparative IS study on exciplex OLEDs based on a starburst carbazole derivative as a donor and Bphen as an acceptor, which were fabricated via a layer-by-layer codeposition process. The study revealed the inductive response (negative capacitance) of the interfacial device at +3 V bias, which is due to the negative differential resistance (NDR) effect, suggesting an additional inductive component in the equivalent circuit. Moreover, the capacitance–voltage (C–

V) and transient EL are powerful tools to study carrier mobility^{35,36} and recombination characteristics,³⁷ which were utilized by Wang et al. to analyze the operation mechanism of OLEDs with different concentrations of the TADF emitter 4CzIPN.³⁸ Transient EL measurements in their study unraveled the details of injected carrier recombination in the EML.

Herein, we provide a detailed comparative analysis of photophysical and electrical characterizations on interfacial- and bulk-exciplex OLED devices fabricated with BCzPh as a donor material^{39,40} and CN-T2T as an acceptor material.²³ All these devices were investigated using time-resolved photoluminescence (TRPL) measurements from short to long wavelengths, impedance spectroscopic (IS) measurements such as the complex-*z* plot and the capacitance–voltage (C–V) plot, and transient electroluminescence (EL) measurements. These comparative studies help us to analyze the exciplex-forming mechanism in detail for a highly efficient exciplex-based OLED device. The results imply that the amount of charge density accumulated at the EML’s interface responsible for exciplex emission is crucial for the EL efficiency. In addition, a clear profile of the delayed fluorescence within the device was confirmed by photophysical and electrical characterizations. Based on these results, we strongly believe that the efficiency of the exciplex-based TADF OLED can be further improved if we can further reduce the accumulated charge in the EML.

■ RESULT AND DISCUSSION

In our previous work, we have demonstrated the BCzPh:CN-T2T blend as an efficient exciplex emitter for achieving good device performance.²⁸ The same materials were utilized in this work for an in-depth comparative study between the interfacial- (BCzPh/CN-T2T) and bulk-exciplex (BCzPh:CN-T2T of 1:1) devices, as depicted in Figure 1.

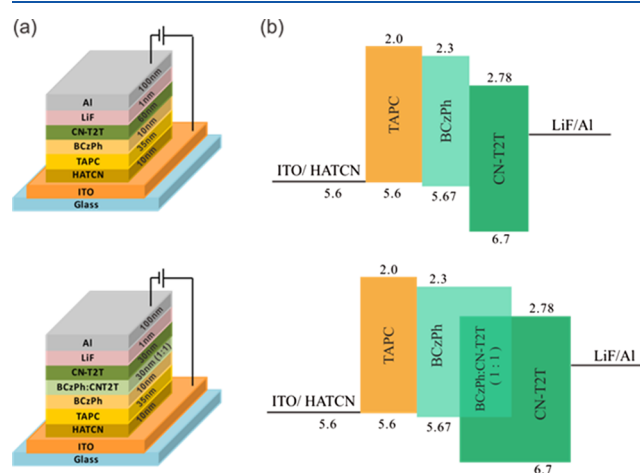


Figure 1. (a) Device structures of the (up) interfacial exciplex and (down) bulk exciplex. (b) Energy level and chemical structures of the (up) interfacial exciplex and (down) bulk exciplex.

The electroluminescence characteristics of our devices are displayed in the current–voltage–luminance profiles, as presented in Figure 2. The performances of these devices are summarized in Table 1. The BCzPh/CN-T2T (interfacial exciplex) device shows a maximum luminance (I_{\max}) at +8 V and reaches up to 5844 cd m⁻² with a Commission

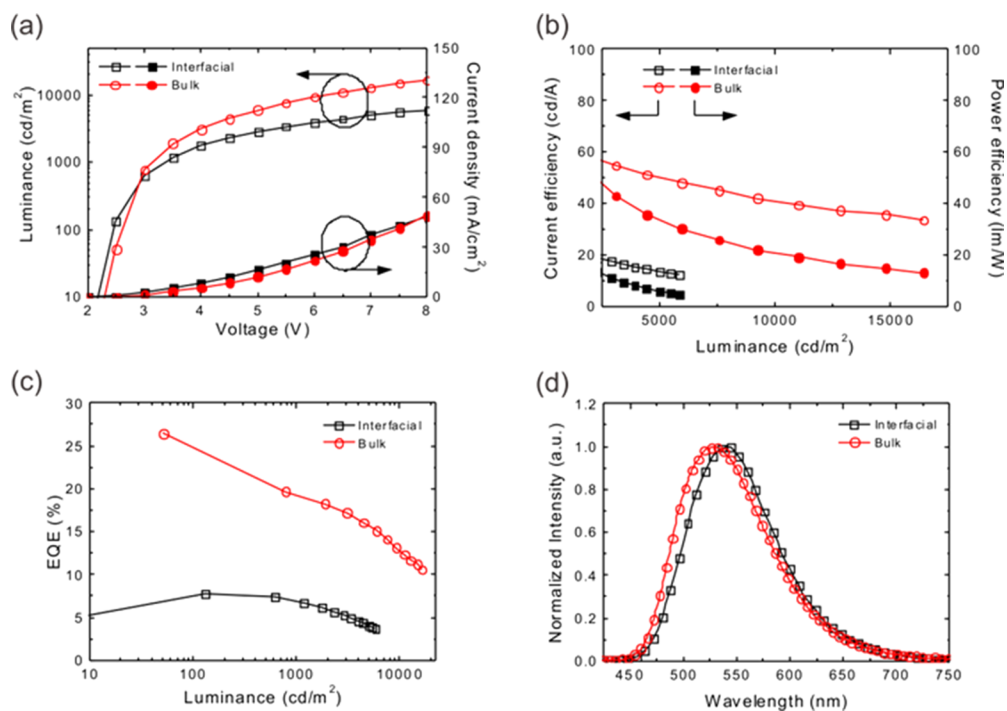


Figure 2. (a) Current density–voltage–luminance, (b) current efficiency–luminance–power efficiency, (c) EQE, and (d) EL spectrum of the interfacial- and bulk-excimer devices.

Table 1. Device Performances of Interfacial and Bulk Devices

	V_{on}	L_{max} (cd m ⁻²)	$\eta_{L,max}$ (cd A ⁻¹)	$\eta_{P,max}$ (lm W ⁻¹)	$\eta_{ext,max}$ (%)	$\lambda_{max,EL}$ (nm)	CIE	1000 cd m ⁻²		10,000 cd m ⁻²	
								η_L (cd A ⁻¹)	η_{ext} (%)	η_L (cd A ⁻¹)	η_{ext} (%)
Interfacial	2.5	5844	25.5	32.1	7.7	540		22.5	6.7	N/A	N/A
Bulk	2.5	16,416	61.5	77.3	26.4	529	(0.33, 0.56)	61.3	19.3	40.8	12.8

Internationale de L'éclairage (CIE) coordinate of (0.36, 0.57). The performance of the device based on the interfacial excimer for the maximum current efficiency (CE), power efficiency (PE), and EQE is 25.5 cd A⁻¹, 32.1 lm W⁻¹, and 7.7%, respectively.

Note that such an interfacial excimer with the optimal structure and thickness was used to achieve better performance, and the details of the different structures can be found in the Supporting Information (Tables S1 and S2). In contrast, the BCzPh:CN-T2T (bulk excimer) device shows an L_{max} at +8 V and reaches up to 16,416 cd m⁻² with a CIE coordinate of (0.33, 0.56). The performance of the device based on the bulk excimer for the maximum CE, PE, and EQE is 61.5 cd A⁻¹, 77.3 lm W⁻¹, and 26.4%, respectively, which indicates the best EQE of excimer-based OLEDs so far. To confirm the reproducibility of highest EQE data, we summarized all measured results of the excimer device from 0 to 3 V in Figure S1. Obviously, the bulk excimer OLED shows remarkably higher EL performance (average highest EQE of ~25.88%) than the counterpart device employing the interfacial excimer. This result can be attributed to the improved recombination efficiency in the EML resulting from the increased intermolecular contacts.²⁶

Interestingly, by comparing these two kinds of devices, the current densities are almost the same, while the EL efficiencies are significantly different (see Figure 2a–c). In Figure 2c, an obvious roll-off is observed for the device with the bulk excimer as compared to the one with the interfacial excimer.

This is possibly attributed to the fact that the bulk excimer exhibits higher propensity for the effective carrier recombination in the EML. However, the Adachi group pointed out that a lot of charge carriers existing in the EML might produce exciton quenching, i.e., singlet–triplet annihilation (STA) or triplet–triplet annihilation (TTA),⁴¹ resulting in the limitation of the device performance. It is easy to see from Figure 2d that the EL emission profiles are dissimilar to each other and show a peak wavelength at 540 nm with a full width at half maximum (FWHM) of 96 nm for the interfacial excimer device and 529 nm with an FWHM of 100 nm for the bulk excimer device. The slight changes in the peak wavelength and the FWHM of the EL spectra suggest the possible contribution of the cavity effect arising from the different emission zones of the devices.^{42,43} This assumption is plausible since the emission is from the donor–acceptor layer junction in the interfacial excimer system and throughout the EML layer in the bulk excimer system. However, an insightful photophysical analysis of the devices is required to investigate the origin of the emission in detail, which has been addressed in this study carefully.

Photoluminescence (PL) Measurement. The steady-state absorption and emission (Figure 3a) of the individual donor and acceptor materials, i.e., BCzPh and CN-T2T, as well as the interfacial (BCzPh/CN-T2T) and bulk (BCzPh:CN-T2T) layers, have been measured to confirm the excimer formation in the devices. The emissions from the individual donor and acceptor molecules show a peak around 405 nm

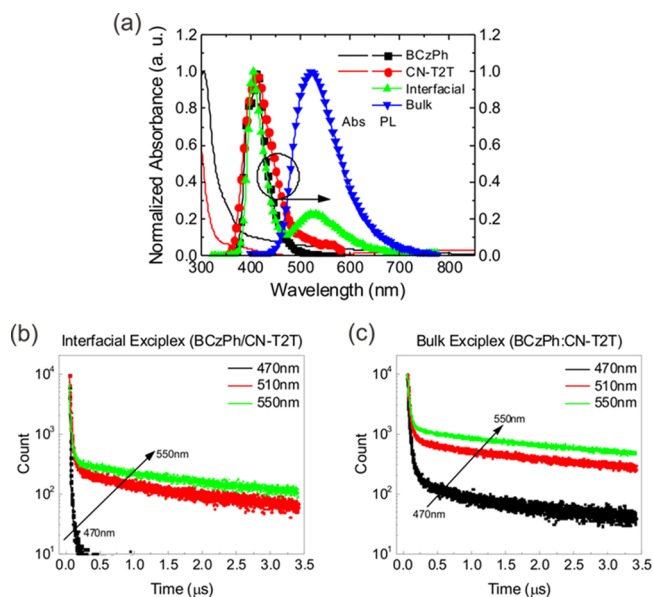


Figure 3. (a) Absorption and PL spectra of BCzPh, CN-T2T, BCzPh/CN-T2T, and BCzPh:CN-T2T thin films. The TRPL decay curve of (b) interfacial and (c) bulk exciplexes.

while the bulk layer (BCzPh:CN-T2T) exhibits a distinct PL peak at 525 nm without showing any peak or hump corresponding to those of the component materials, which explicitly indicates efficient exciplex formation in the device. On the other hand, the emission from the interfacial (BCzPh/CN-T2T) layer shows a prominent PL peak at 405 nm and comparatively a less intense peak at 525 nm, indicating insufficient exciplex formation at the junction of the donor and acceptor layers. As a consequence, the bulk exciplex device outperforms the interfacial exciplex device, which is also corroborated by the electroluminescence data shown in Figure 2.

Time-resolved photoluminescence (TRPL) measurements from short to long wavelengths were carried out to investigate the efficient harvest of nonradiative triplet excitons into singlet excitons via reverse intersystem crossing as well as to monitor the delayed fluorescence of the device. As monitored at longer wavelengths in the delayed fluorescence, the $D^{\bullet} \rightarrow A^{\bullet}$ dipole is smaller, and therefore, the electron cloud gets more deformed, resulting in increased spin-orbit coupling and a decrease in the singlet–triplet energy gap (ΔE_{ST}) of the exciplex.²⁸ That is why an efficient delayed fluorescence is expected at longer wavelengths for both the exciplex devices, as shown in Figure 3b,c. The TRPL profiles of the interfacial and bulk exciplex devices show two decay regions: a short-prompt fluorescence region and a long-delayed fluorescence region, which are fitted to an exponential function to extract the decay times, as presented in Table 2. As a result, the numbers of counts of delayed fluorescence for the bulk exciplex are far larger than those of prompt fluorescence at any excitation wavelengths as compared with the interfacial exciplex. This result provides direct evidence indicating that the bulk system could induce more heterointerface regions in the EML, resulting in the improvement of exciplex emission efficiency.

The bulk exciplex device shows delayed fluorescence in the order of microseconds irrespective of the detecting PL wavelengths, i.e., 470, 510, and 550 nm. On the contrary, the interfacial exciplex device shows a very short delayed

Table 2. Summary of Fitting Parameters of the TRPL Decay Profiles for Interfacial and Bulk Exciplex Films

	emission wavelength (nm)	T_1 (ns)	T_2 (ns)
interfacial	470	3.04	42.69
	510	14.07	913.44
	550	16.06	1282.01
bulk	470	19.01	687.84
	510	26.98	1377.93
	550	27.75	1644.87

fluorescence (~ 42 ns) at a wavelength of 470 nm. Upon increasing the wavelength to 550 nm, the delayed fluorescence (~ 1.2 μ s) of the interfacial exciplex was lower than that of the bulk exciplex (~ 1.6 μ s), indicating insufficient exciplex formation within the device. This result implies that the total amount of BCzPh/CN-T2T interfaces is the primary factor in determining the efficiency of exciplex emission, and thus, it explains why the bulk exciplex device outperforms the interfacial exciplex one.

Impedance Spectroscopy Measurement. The dynamics of mobile charges, as well as interfacial charges, are analyzed by studying the C – V characteristics of the devices. Four different bias conditions could be distinguished from the mobile charge dynamics in the C – V plots. At an applied bias (V_0) less than the threshold bias (V_t) condition, i.e., $V_0 < V_t$, the charge carriers are not injected into the devices, and the device behaves like an insulating dielectric between two electrodes. As a consequence, the capacitance value of the device under these conditions would be constant, and the value corresponds to the geometric capacitance.⁴⁴ While V_0 crosses V_t but lower than the built-in voltage (V_{bi}), i.e., $V_t < V_0 < V_{bi}$, the holes start to get injected into the device, increasing the capacitance as the holes get accumulated in the device. The capacitance value keeps increasing with V_0 until it reaches V_{bi} , i.e., $V_0 = V_{bi}$. For $V_0 > V_{bi}$, the injection of electrons is initiated, and the electron–hole recombination takes place, resulting in a decrease in the capacitance due to the decrease in the accumulated charge carriers in the device.

For a comparative study, the C – V plots of the interfacial- and bulk-exciplex devices are shown in Figure 4. At the

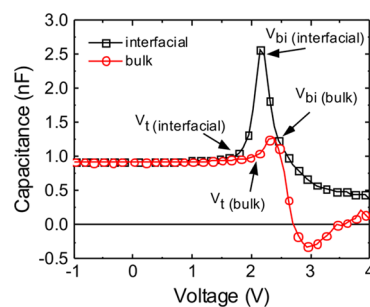


Figure 4. Capacitance–voltage characteristics of the devices with interfacial and bulk exciplexes.

condition of $V_0 < V_t$, the capacitance remains constant with the value corresponding to the geometrical capacitance. The capacitance value of both devices is similar since the thickness of the devices is almost equal. For example, the capacitance values are 0.94 and 0.93 nF for the interfacial and bulk exciplex, respectively. For $V_0 > V_t$, the capacitance value starts to increase for both the devices as expected and reaches the

maximum value at $V_0 = V_{bi}$. The V_t and V_{bi} were determined to be around 1.71 and 2.15 V for interfacial exciplex and around 2.06 and 2.38 V for the bulk exciplex. It is noteworthy that the V_t and V_{bi} values of the bulk exciplex device are slightly higher than those of the interfacial exciplex device. This implies that a higher energy is required to inject the carriers into the bulk exciplex device compared to the interfacial exciplex device, which could be justified by considering the thicker emission layer of the bulk exciplex device. Besides, the key finding is that the bulk exciplex (capacitance = 1.28 nF at V_{bi}) shows a lower-charge accumulation profile due to its broad emission zone, which could smoothen the charge distribution in the EML as compared to that (capacitance = 2.57 nF at V_{bi}) of the interfacial exciplex.

At $V_0 > V_{bi}$, the recombination process is initiated, and the capacitance value decreases for both the devices. The capacitance of the bulk exciplex device is decreased to a much lower value than that of the interfacial exciplex device, which could be attributed to its large recombination area in the EML. Interestingly, the capacitance of the bulk exciplex device decreases to negative values. Negative capacitance values have been reported under bipolar injection conditions where recombination occurs through localized trap states.^{45,46} Bisquert et al. observed a negative capacitance at a lower frequency in OLEDs. Such a negative capacitance response was caused by electron injection at the organic/metal interface through the interfacial states in the bandgap. The increased rate of hopping to the bulk states results in the negative capacitance of the device.⁴⁷ Guan et al. pointed out that the $C-V$ curve is affected by the carrier injection rate and consumption rate i.e., the higher C value resulted from the faster carrier injection rate than the carrier consumption rate. The negative capacitance was also reported as a consequence of the synchronized change of the internal accumulated carrier's transport states, and the applied small ac signal arises from the differences in the mobility of carriers in organic layers.⁴⁸ The summary values for the equivalent circuit models are listed in the Supporting Information (Figure S2 and Table S3).

The complex- z plot is often used for extracting the RC component in an OLED's equivalent circuit. Figure 5 shows

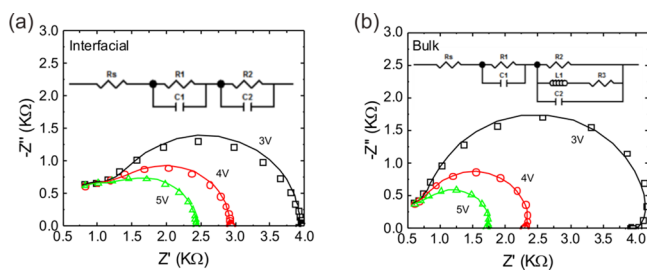


Figure 5. Complex- z and the equivalent circuit of the devices with (a) interfacial exciplex and (b) bulk exciplex.

the interfacial- and bulk-exciplex device complex- z plots. The minimum Z' value in the plot represents the contact resistance at the electrodes and is displayed as the series resistance in the equivalent circuit. The sum of the series resistance and the parallel resistance in the parallel RC circuit corresponds to the maximum Z' value.⁴⁹ The size of the semicircle in the complex- z plot for the bulk exciplex device was observed to be larger than that in the interfacial exciplex device at an applied bias of

+3 V. The maximum Z' and Z'' values of the bulk exciplex (interfacial exciplex) of 4.16 (3.95) and 1.70 (1.31) K Ω , respectively were obtained. Moreover, it should be noted that the sizes of the semicircles for the bulk exciplex device decrease more compared to those of the interfacial exciplex device as the applied bias increases. For example, when we applied a bias voltage of +5.0 V, maximum Z' and Z'' values of the bulk exciplex (interfacial exciplex) 1.74 (2.43) and 0.58 (0.73) K Ω , respectively, were obtained. This observation is in agreement with the $C-V$ behavior of the devices.

As shown in the complex- z plot, the equivalent circuit of the interfacial device can be represented as a series connection of two parallel RC circuits along with a series of contact resistance. Two parallel RC circuits serve the purpose of two different electrical transport phenomena in OLEDs.⁵⁰ One parallel RC (R_{p1} , C_{p1}) circuit stands for the resistance and the capacitance of the hole-conduction layer, and the other parallel RC (R_{p2} , C_{p2}) circuit represents the same for the electron-conduction layer. The series resistance (R_s) in the equivalent circuit defines the contact resistance between the semiconductor and the metal.⁵¹ In contrast, the bulk exciplex device exhibits a negative capacitance or an inductive response at a lower frequency. Accordingly, an inductance (L) is incorporated into the parallel RC circuit in the equivalent circuit of the bulk exciplex device. The fitting parameters of the equivalent circuits for each device at different bias voltages are listed in Table 3. The parameters of R_s for the bulk exciplex (319.2 Ω) and interfacial exciplex (307.6 Ω) were similar values. This result indicates that the contact resistance between the semiconductor and the metal in the bulk and interfacial exciplex is the same. The values of R_1 , C_1 , R_2 , and C_2 decrease with the increase in the applied bias, and the decrease is more severe for the bulk exciplex device because of more hole and electron injection to the device. When the bias voltage increases from +3.0 to +5.0 V, the loss value of C_2 of the bulk exciplex (0.13 nF) is much higher than that (0.06 nF) of the interfacial exciplex. That is why the bulk exciplex device exhibits a higher EL efficiency.

Transient Electroluminescence Measurement. Recently, Han et al. investigated the effect of hole-injection on the degradation mechanism of OLEDs by transient electroluminescence.^{35,36} The result showed that the transient EL is a reliable tool to study the charge injection and transportation in the device. The rising and delay times in the transient EL were observed to increase, which is an indication of the degradation in the EML. The reduction in carrier injection or transportation was attributed to the inefficient hole injection layer. Finally, a reduced energy barrier to the HIL was suggested to decrease the rising time and delay time. However, the above reference guides us to inspect the spike or overshoot response in the decayed part of the EL data for an informative analysis of the recombination zone in the device. The decay time (after turning off the voltage pulse) could reveal the dynamics of carrier depletion inside the emitting layer. On the other hand, the dynamics of the trapped charges in the recombination area can be analyzed by studying the overshoot responses carefully.^{52,53}

The transient EL measurement was carried out to investigate trapped charges inside the interfacial- and bulk-exciplex devices. Figure 6 shows the transient EL decay profile of the interfacial and bulk exciplex OLEDs for comparison. In the EL decay measurement, a reverse bias was applied to extract charge carriers from the emission layer. The overshoot in the

Table 3. Summary of Equivalent Circuit Data of Interfacial and Bulk Devices

	voltage (V)	R_s (Ω)	R_1 (Ω) (%)	C_1 (nF) (%)	R_2 (Ω) (%)	C_2 (nF) (%)	L_1 (H) (%)	R_3 (Ω) (%)
interfacial	3	319.2	949.7 \pm 1.79	0.17 \pm 4.93	2668 \pm 0.50	1.05 \pm 1.40		
	4	319.2	917.4 \pm 0.81	0.17 \pm 0.82	1683 \pm 0.45	1.00 \pm 1.26		
	5	319.2	918.2 \pm 0.82	0.17 \pm 0.58	1193 \pm 0.63	0.99 \pm 1.51		
bulk	3t	307.6	465.5 \pm 2.98	0.30 \pm 7.97	3453 \pm 0.45	1.06 \pm 0.80	2.14 \pm 14.11	35,064 \pm 5.25%
	4t	307.6	414.3 \pm 0.65	0.28 \pm 0.87	1675 \pm 0.22	0.95 \pm 0.54	0.39 \pm 9.48	24,371 \pm 3.64%
	5t	307.6	415.3 \pm 0.99	0.29 \pm 0.80	1062 \pm 0.35	0.93 \pm 1.01	0.12 \pm 10.73	14,473 \pm 4.37%

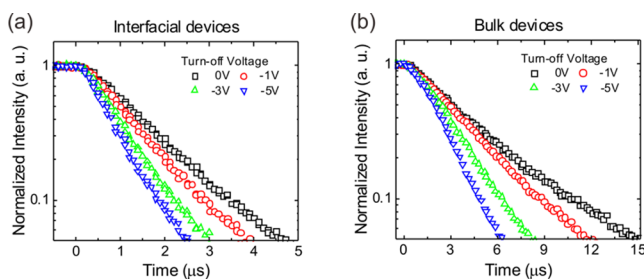


Figure 6. Transient EL profile of (a) interfacial exciplex and (b) bulk exciplex devices at the decayed part, depending on the given reverse bias at 0, -1, -3, and -5 V.

decay profile is explained, in general, by the recombination of the trap charges with the residual charges inside the emission layer. No overshoot is observed in the decay profile of the interfacial- and bulk-exciplex device, ruling out the existence of any trapped charges in the EML. In contrast, the recombination type of both devices is confirmed to be Langevin recombination. The longer decay time at the bulk exciplex is due to the fact that plenty of charge carriers remained inside the emission layer after the applied reverse bias is turned off, leading to higher delayed fluorescence inside the bulk exciplex compared to the interfacial exciplex. The decay time of the bulk exciplex device is strongly reduced compared to that of the interfacial exciplex device at an applied reverse bias. We have reported in our previous work that the faster-reduced decay corresponds to no or less trapped charge carriers inside the emission layer and the charge carriers can recombine efficiently after the applied bias is turned off.³⁹ The shorter decay time of the interfacial exciplex is because fewer charge carriers remained in the interfacial layer. Thus, the transient EL decay profile explains clearly the higher EL efficiency of the bulk exciplex device as compared to the interfacial exciplex device.

CONCLUSIONS

In this work, we report a comparative photophysical and electrical analysis of exciplex-based devices with emission from the BCzPh/CN-T2T interfacial layer or the BCzPh:CN-T2T bulk layer. The emission spectrum shows that the bulk exciplex device exhibits an exciplex-only emission, whereas the primary emission from the interfacial exciplex device arises from the CN-T2T layer and a minor contribution from the exciplex emission. The bulk exciplex device displays a clear profile of delayed fluorescence as compared to the interfacial exciplex device. The electrical characterizations clarify that the higher EL efficiency of the bulk exciplex device is contributed from the lower values of R_{p1} , C_{p1} , R_{p2} , and C_{p2} . The well-mixed donor-acceptor junction that leads to an increased recombination zone mainly leads to a lower capacitance at the bulk exciplex. The observed longer decay time of the bulk exciplex

device in the transient EL measurement indicates that plenty of charge carriers remain in the emission layer, resulting in delayed fluorescence. In addition, the EL decay time of the bulk exciplex device is strongly reduced upon applying a reverse bias, which implies that there are no trapped charge carriers in the emission layer i.e., the charge carriers recombine faster after the applied bias is turned off. In contrast, the shorter EL decay time of the interfacial exciplex device is because fewer charge carriers remain at the interfacial layer. We believe that the detailed photophysical and electrical characterizations of the interfacial and bulk exciplex devices reported in this work will benefit research studies on the development of new organic materials as well as device configuration for advancing a step further to achieve more efficient exciplex-based OLED devices.

EXPERIMENTAL SECTION

OLED Device Fabrication and Measurement. Organic materials, 1,4,5,8,9,11-hexaazatriphenylene hexacarbonitrile (HATCN), di-[4-(N,N-di-437 tolylamino)-phenyl]cyclohexane (TAPC), and 9,9'-diphenyl-9H,9'H-3,3'-bicarbazole (BCzPh) were purchased from Shine Materials Technology Co. Ltd. 3',3''',3''''-(1,3,5-triazine-2,4,6-triyl)tris((1,1'-biphenyl)-3-carbonitrile) (CN-T2T) was synthesized in the laboratory. All the organic materials were sublimated using a homemade purification system under high vacuum conditions before the device fabrication. Our proposed devices were fabricated with the structure of ITO/HATCN (7.5 nm)/TAPC (35 nm)/BCzPh (10 nm)/CN-T2T (60 nm)/LiF (1 nm)/Al (100 nm) for interfacial exciplex devices and the structure of ITO/HATCN (7.5 nm)/TAPC (35 nm)/BCzPh (10 nm)/BCzPh:CN-T2T (30 nm; 1:1)/CN-T2T (30 nm)/LiF (1 nm)/Al (100 nm) for bulk exciplex devices. Deionized (DI) water, acetone, and isopropyl alcohol were used to clean the ITO substrate in an ultrasonic bath. Note that such ITO was prepared by using a sputter under room temperature conditions to deposit a 70 nm thick transparent conduction oxide layer as an anode in which the sheet resistance is $90 \Omega^{-2}$ and the transmittance value is $>92\%$ at 515 nm. The ITO substrate was then dried using a nitrogen (N_2) blower. The thickness of the deposited materials was measured using a surface profiler (Dektak XT). The ITO substrate was transferred to a thermal evaporation system to deposit organic layers and metal electrodes. To achieve a highly smooth morphology, the pressure was kept at a high-vacuum level of 2×10^{-6} Torr, and the deposition rate was controlled around $0.5-1 \text{ \AA s}^{-1}$. At the final step, the devices were encapsulated with a glass substrate in the glove box under moisture conditions of <0.1 ppm. Current density-voltage-luminance ($J-V-L$) measurements were performed using a spectrum scan PR655 and a Keithley 2400 source meter.

Photophysical Measurement. The steady-state optical absorption and emission and time-resolved photoluminescence (TRPL) were measured in a nitrogen-filled chamber using a spectrofluorometer (FluoroMax Plus, HORIBA Jobin Yvon). In the steady-state absorption and emission, the thin-film sample was studied at an excitation wavelength of 305 nm using an ozone-free xenon arc lamp under ambient conditions. In the TRPL measurement, all photoluminescence decays were measured using a NanoLED pulsed diode

controller (N-320, HORIBA Jobin Yvon) at an excitation wavelength of 320 nm with a pulse frequency of 50 kHz.

Electrical Measurement. Impedance Spectroscopy. Impedance spectroscopy (IS) measurements and analysis were performed using an XM SOLARTRON analytical (Material Lab). The complex- z plot was obtained using frequency sweep values ranging from 1 Hz to 1 MHz at bias voltages of +3, +4, and +5 V. The capacitance–voltage ($C-V$) plot was obtained using voltage sweep values ranging from -1 to +5 V under a frequency of 1 kHz. The amplitude of the AC oscillator level was set to 50 mV for all the impedance spectroscopic measurements.

Transient Electroluminescence. Transient electroluminescence (EL) measurements were performed using a Tektronix AFG 3102C function generator connected to a South Port optical detector. PicoQuant FluoFit software was used to analyze the data. A square voltage pulse was supplied to the devices from a function generator delivering a voltage pulse width of 100 μ s, pulse height corresponding to 10 mA cm^{-2} , and a pulse frequency of 100 Hz. The measurement was carried out at the reverse bias after turning off the voltage pulse at 0, -1 , -3 , and -5 V.

■ ASSOCIATED CONTENT

Supporting Information

The Supporting Information is available free of charge at <https://pubs.acs.org/doi/10.1021/acsaelm.0c00062>.

The testing recipes of the interfacial exciplex; the EL characterizations of the interfacial exciplex; the reproducibility of the exciplex's EQE data; the parameters of the exciplex's equivalent circuit for the interfacial and bulk exciplexes; the CV measurements of the interfacial and bulk exciplexes (PDF).

■ AUTHOR INFORMATION

Corresponding Authors

Shun-Wei Liu – Department of Electronic Engineering and Organic Electronics Research Center, Ming Chi University of Technology, New Taipei City 24301, Taiwan; orcid.org/0000-0002-3128-905X; Email: swliu@mail.mcut.edu.tw

Ken-Tsung Wong – Department of Chemistry, National Taiwan University, Taipei 10617, Taiwan; Institute of Atomic and Molecular Science, Academia Sinica, Taipei 10617, Taiwan; orcid.org/0000-0002-1680-6186; Email: kenwong@ntu.edu.tw

Authors

Nurul Ridho Al Amin – Department of Electronic Engineering and Organic Electronics Research Center, Ming Chi University of Technology, New Taipei City 24301, Taiwan; Department of Electronic Engineering, National Taiwan University of Science and Technology, Taipei 10617, Taiwan

Kiran Kishore Kesavan – Department of Electronic Engineering and Organic Electronics Research Center, Ming Chi University of Technology, New Taipei City 24301, Taiwan

Sajal Biring – Department of Electronic Engineering and Organic Electronics Research Center, Ming Chi University of Technology, New Taipei City 24301, Taiwan

Chih-Chien Lee – Department of Electronic Engineering, National Taiwan University of Science and Technology, Taipei 10617, Taiwan

Tzu-Hung Yeh – Department of Electronic Engineering, National Taiwan University of Science and Technology, Taipei 10617, Taiwan

Tzu-Yu Ko – Department of Chemistry, National Taiwan University, Taipei 10617, Taiwan

Complete contact information is available at:
<https://pubs.acs.org/10.1021/acsaelm.0c00062>

Notes

The authors declare no competing financial interest.

■ ACKNOWLEDGMENTS

The authors acknowledge financial support from the Ministry of Science and Technology (Grant Nos. MOST 107-2113-M-002-019-MY3, 107-2221-E-131-029-MY2, 107-2119-M-131-001, 108-2221-E-131-027-MY2, and 108-2221-E-011-151). Also, the corresponding author (S.-W. Liu) is grateful to Mr. H.-H. Wu, Syskey Technology Corporation (Taiwan), for his assistance in designing the fabrication system.

■ REFERENCES

- (1) Zhao, B.; Liu, Z.; Wang, Z.; Zhang, H.; Li, J.; Wang, H.; Xu, B.; Wu, Y.; Li, W. Structural Design for Highly Efficient Pure Fluorescent Warm WOLEDs by Employing TADF Molecule as Blue Emitter and Exciplex Donor. *Org. Electron.* **2019**, *73*, 1–6.
- (2) Zhang, T.; Zhao, B.; Chu, B.; Li, W.; Su, Z.; Yan, X.; Liu, C.; Wu, H.; Gao, Y.; Jin, F.; Hou, F. Simple Structured Hybrid WOLEDs Based on Incomplete Energy Transfer Mechanism: From Blue Exciplex to Orange Dopant. *Sci. Rep.* **2015**, *5*, 10234.
- (3) Uoyama, H.; Goushi, K.; Shizu, K.; Nomura, H.; Adachi, C. Highly Efficient Organic Light-Emitting Diodes from Delayed Fluorescence. *Nature* **2012**, *492*, 234–238.
- (4) Kaji, H.; Suzuki, H.; Fukushima, T.; Shizu, K.; Suzuki, K.; Kubo, S.; Komino, T.; Oiwa, H.; Suzuki, F.; Wakamiya, A.; Murata, Y.; Adachi, C. Purely Organic Electroluminescent Material Realizing 100% Conversion from Electricity to Light. *Nat. Commun.* **2015**, *6*, 8476.
- (5) Lin, T.-A.; Chatterjee, T.; Tsai, W.-L.; Lee, W.-K.; Wu, M.-J.; Jiao, M.; Pan, K.-C.; Yi, C.-L.; Chung, C.-L.; Wong, K.-T.; Wu, C.-C. Sky-Blue Organic Light Emitting Diode with 37% External Quantum Efficiency Using Thermally Activated Delayed Fluorescence from Spiroacridine-Triazine Hybrid. *Adv. Mater.* **2016**, *28*, 6976–6983.
- (6) Colella, M.; Danos, A.; Monkman, A. P. Less Is More: Dilution Enhances Optical and Electrical Performance of a TADF Exciplex. *J. Phys. Chem. Lett.* **2019**, *10*, 793–798.
- (7) Gao, K.; Liu, K.; Li, X.-L.; Cai, X.; Chen, D.; Xu, Z.; He, Z.; Li, B.; Qiao, Z.; Chen, D.; Cao, Y.; Su, S.-J. An Ideal Universal Host for Highly Efficient Full-Color, White Phosphorescent and TADF OLEDs with a Simple and Unified Structure. *J. Mater. Chem. C* **2017**, *5*, 10406–10416.
- (8) Kato, Y.; Sasabe, H.; Hayasaka, Y.; Watanabe, Y.; Arai, H.; Kido, J. A Sky Blue Thermally Activated Delayed Fluorescence Emitter to Achieve Efficient White Light Emission through in Situ Metal Complex Formation. *J. Mater. Chem. C* **2019**, *7*, 3146–3149.
- (9) Jankus, V.; Data, P.; Graves, D.; McGuinness, C.; Santos, J.; Bryce, M. R.; Dias, F. B.; Monkman, A. P. Highly Efficient TADF OLEDs: How the Emitter-Host Interaction Controls Both the Excited State Species and Electrical Properties of the Devices to Achieve near 100% Triplet Harvesting and High Efficiency. *Adv. Funct. Mater.* **2014**, *24*, 6178–6186.
- (10) Tao, Y.; Yuan, K.; Chen, T.; Xu, P.; Li, H.; Chen, R.; Zheng, C.; Zhang, L.; Huang, W. Thermally Activated Delayed Fluorescence Materials towards the Breakthrough of Organoelectronics. *Adv. Mater.* **2014**, *26*, 7931–7958.
- (11) Goushi, K.; Adachi, C. Efficient Organic Light-Emitting Diodes through up-Conversion from Triplet to Singlet Excited States of Exciplexes. *Appl. Phys. Lett.* **2012**, *101*, No. 023306.
- (12) Yang, Z.; Mao, Z.; Xie, Z.; Zhang, Y.; Liu, S.; Zhao, J.; Xu, J.; Chi, Z.; Aldred, M. P. Recent Advances in Organic Thermally Activated Delayed Fluorescence Materials. *Chem. Soc. Rev.* **2017**, *46*, 915–1016.

- (13) Godumala, M.; Choi, S.; Cho, M. J.; Choi, D. H. Recent Breakthroughs in Thermally Activated Delayed Fluorescence Organic Light Emitting Diodes Containing Non-Doped Emitting Layers. *J. Mater. Chem. C* **2019**, *7*, 2172–2198.
- (14) Ahn, D. H.; Kim, S. W.; Lee, H.; Ko, I. J.; Karthik, D.; Lee, J. Y.; Kwon, J. H. Highly Efficient Blue Thermally Activated Delayed Fluorescence Emitters Based on Symmetrical and Rigid Oxygen-Bridged Boron Acceptors. *Nat. Photonics* **2019**, *13*, 540–546.
- (15) Goushi, K.; Yoshida, K.; Sato, K.; Adachi, C. Organic Light-Emitting Diodes Employing Efficient Reverse Intersystem Crossing for Triplet-to-Singlet State Conversion. *Nat. Photonics* **2012**, *6*, 253–258.
- (16) Lee, S.; Kim, K. H.; Limbach, D.; Park, Y. S.; Kim, J. J. Low Roll-off and High Efficiency Orange Organic Light Emitting Diodes with Controlled Co-Doping of Green and Red Phosphorescent Dopants in an Exciplex Forming Co-Host. *Adv. Funct. Mater.* **2013**, *23*, 4105–4110.
- (17) Chapran, M.; Angioni, E.; Findlay, N. J.; Breig, B.; Cherpak, V.; Stakhira, P.; Tuttle, T.; Volyniuk, D.; Grazulevicius, J. V.; Nastishin, Y. A.; Lavrentovich, O. D.; Skabara, P. J. An Ambipolar BODIPY Derivative for a White Exciplex OLED and Cholesteric Liquid Crystal Laser toward Multifunctional Devices. *ACS Appl. Mater. Interfaces* **2017**, *9*, 4750–4757.
- (18) Endo, A.; Sato, K.; Yoshimura, K.; Kai, T.; Kawada, A.; Miyazaki, H.; Adachi, C. Efficient up-Conversion of Triplet Excitons into a Singlet State and Its Application for Organic Light Emitting Diodes. *Appl. Phys. Lett.* **2011**, *98*, No. 083302.
- (19) Kalinowski, J. Excimers and Exciplexes in Organic Electroluminescence. *Mater. Sci.* **2009**, *27*, 735–756.
- (20) Liu, X.-K.; Chen, Z.; Zheng, C.-J.; Liu, C.-L.; Lee, C.-S.; Li, F.; Ou, X.-M.; Zhang, X.-H. Prediction and Design of Efficient Exciplex Emitters for High-Efficiency, Thermally Activated Delayed-Fluorescence Organic Light-Emitting Diodes. *Adv. Mater.* **2015**, *27*, 2378–2383.
- (21) Chen, D.; Liu, K.; Gan, L.; Liu, M.; Gao, K.; Xie, G.; Ma, Y.; Cao, Y.; Su, S. J. Modulation of Exciton Generation in Organic Active Planar Pn Heterojunction: Toward Low Driving Voltage and High-Efficiency OLEDs Employing Conventional and Thermally Activated Delayed Fluorescent Emitters. *Adv. Mater.* **2016**, *28*, 6758–6765.
- (22) Wu, T.-L.; Liao, S.-Y.; Huang, P.-Y.; Hong, Z.-S.; Huang, M.-P.; Lin, C.-C.; Cheng, M.-J.; Cheng, C.-H. Exciplex Organic Light-Emitting Diodes with Nearly 20% External Quantum Efficiency: Effect of Intermolecular Steric Hindrance between the Donor and Acceptor Pair. *ACS Appl. Mater. Interfaces* **2019**, *11*, 19294–19300.
- (23) Hung, W. Y.; Chiang, P. Y.; Lin, S. W.; Tang, W. C.; Chen, Y. T.; Liu, S. H.; Chou, P. T.; Hung, Y. T.; Wong, K. T. Balance the Carrier Mobility to Achieve High Performance Exciplex OLED Using a Triazine-Based Acceptor. *ACS Appl. Mater. Interfaces* **2016**, *8*, 4811–4818.
- (24) Liang, B.; Wang, J.; Cheng, Z.; Wei, J.; Wang, Y. Exciplex-Based Electroluminescence: Over 21% External Quantum Efficiency and Approaching 100 lm/W Power Efficiency. *J. Phys. Chem. Lett.* **2019**, *10*, 2811–2816.
- (25) Hung, W.-Y.; Fang, G.-G.; Chang, Y.-C.; Kuo, T.-Y.; Chou, P.-T.; Lin, S.-W.; Wong, K.-T. Highly Efficient Bilayer Interface Exciplex For Yellow Organic Light-Emitting Diode. *ACS Appl. Mater. Interfaces* **2013**, *5*, 6826–6831.
- (26) Hung, W. Y.; Fang, G. C.; Lin, S. W.; Cheng, S. H.; Wong, K. T.; Kuo, T. Y.; Chou, P. T. The First Tandem, All-Exciplex-Based WOLED. *Sci. Rep.* **2014**, *4*, 5161.
- (27) Chapran, M.; Pander, P.; Vasylieva, M.; Wiosna-Salyga, G.; Ulanski, J.; Dias, F. B.; Data, P. Realizing 20% External Quantum Efficiency in Electroluminescence with Efficient Thermally Activated Delayed Fluorescence from an Exciplex. *ACS Appl. Mater. Interfaces* **2019**, *11*, 13460–13471.
- (28) Wang, M.; Huang, Y.-H.; Lin, K.-S.; Yeh, T.-H.; Duan, J.; Ko, T.-Y.; Liu, S.-W.; Wong, K.-T.; Hu, B. Revealing Cooperative Relationship between Spin, Energy and Polarization Parameters towards Developing High-Efficiency Exciplex Light-Emitting Diodes. *Adv. Mater.* **2019**, *31*, 1904114.
- (29) Zheng, R.; Huang, W.-B.; Xu, W.; Cao, Y. Analysis of Intrinsic Degradation Mechanism in Organic Light-Emitting Diodes by Impedance Spectroscopy. *Chin. Phys. Lett.* **2014**, *31*, No. 027703.
- (30) Okachi, T.; Nagase, T.; Kobayashi, T.; Naito, H. Determination of Charge-Carrier Mobility in Organic Light-Emitting Diodes by Impedance Spectroscopy in Presence of Localized States. *Jpn. J. Appl. Phys.* **2008**, *47*, 8965–8972.
- (31) Nowy, S.; Ren, W.; Wagner, J.; Weber, J. A.; Brütting, W. Impedance Spectroscopy of Organic Hetero-Layer OLEDs as a Probe for Charge Carrier Injection and Device Degradation. *Proc. SPIE* **2009**, *7415*, 74150G.
- (32) Juhasz, P.; Nevrel, J.; Micjan, M.; Novota, M.; Uhrík, J.; Stuchlikova, L.; Jakabovic, J.; Harmatha, L.; Weis, M. Charge Injection and Transport Properties of an Organic Light-Emitting Diode. *Beilstein J. Nanotechnol.* **2016**, *7*, 47–52.
- (33) Park, H.; Kim, H.; Dhungel, S. K.; Yi, J.; Sohn, S. Y.; Jung, D. G. Impedance Spectroscopy Analysis of Organic Light-Emitting Diodes Fabricated on Plasma-Treated Indium-Tin-Oxide Surfaces. *J. Korean Phys. Soc.* **2007**, *51*, 1011–1015.
- (34) Chapran, M.; Ivaniuk, K.; Stakhira, P.; Cherpak, V.; Hotra, Z.; Volyniuk, D.; Michaleviciute, A.; Tomkeviciene, A.; Voznyak, L.; Grazulevicius, J. V. Essential Electro-Optical Differences of Exciplex Type OLEDs Based on a Starburst Carbazole Derivative Prepared by Layer-by-Layer and Codeposition Processes. *Synth. Met.* **2015**, *209*, 173–177.
- (35) Han, T.-H.; Song, W.; Lee, T.-W. Elucidating the Crucial Role of Hole Injection Layer in Degradation of Organic Light-Emitting Diodes. *ACS Appl. Mater. Interfaces* **2015**, *7*, 3117–3125.
- (36) Han, T.-H.; Kim, Y.-H.; Kim, M. H.; Song, W.; Lee, T.-W. Synergetic Influences of Mixed-Host Emitting Layer Structures and Hole Injection Layers on Efficiency and Lifetime of Simplified Phosphorescent Organic Light-Emitting Diodes. *ACS Appl. Mater. Interfaces* **2016**, *8*, 6152–6163.
- (37) Lee, J.-H.; Lee, S.; Yoo, S.-J.; Kim, K.-H.; Kim, J.-J. Langevin and Trap-Assisted Recombination in Phosphorescent Organic Light Emitting Diodes. *Adv. Funct. Mater.* **2014**, *24*, 4681–4688.
- (38) Wang, P.; Zhao, S.; Xu, Z.; Qiao, B.; Long, Z.; Huang, Q. The Electroluminescence Mechanism of Solution-Processed TADF Emitter 4CzIPN Doped OLEDs Investigated by Transient Measurements. *Molecules* **2016**, *21*, 1365.
- (39) Shih, C.-J.; Lee, C.-C.; Yeh, T.-H.; Biring, S.; Kesavan, K. K.; Al Amin, N. R.; Chen, M.-H.; Tang, W.-C.; Liu, S.-W.; Wong, K.-T. Versatile Exciplex-Forming Co-Host for Improving Efficiency and Lifetime of Fluorescent and Phosphorescent Organic Light-Emitting Diodes. *ACS Appl. Mater. Interfaces* **2018**, *10*, 24090–24098.
- (40) Sasabe, H.; Toyota, N.; Nakanishi, H.; Ishizaka, T.; Pu, Y.-J.; Kido, J. 3,3'-Bicarbazole-Based Host Materials for High-Efficiency Blue Phosphorescent OLEDs with Extremely Low Driving Voltage. *Adv. Mater.* **2012**, *24*, 3212–3217.
- (41) Masui, K.; Nakanotani, H.; Adachi, C. Analysis of Exciton Annihilation in High-Efficiency Sky-Blue Organic Light-Emitting Diodes with Thermally Activated Delayed Fluorescence. *Org. Electron.* **2013**, *14*, 2721–2726.
- (42) Chan, J.; Lu, A. W.; Cheung, C. H.; Ng, A. M. C.; Djurišić, A. B.; Yeow, Y. T.; Rakić, A. D. Cavity Design and Optimization for Organic Microcavity OLEDs. *Proc. SPIE* **2006**, *6038*, 603824.
- (43) Poitras, D.; Kuo, C.-C.; Py, C. Design of High-Contrast OLEDs with Microcavity Effect. *Opt. Express* **2008**, *16*, 8003–8015.
- (44) Brütting, W.; Berleb, S.; Mückl, A. G. Device Physics of Organic Light-Emitting Diodes Based on Molecular Materials. *Org. Electron.* **2001**, *2*, 1–36.
- (45) Ehrenfreund, E.; Lungenschmied, C.; Dennler, G.; Neugebauer, H.; Sariciftci, N. S. Negative Capacitance in Organic Semiconductor Devices: Bipolar Injection and Charge Recombination Mechanism. *Appl. Phys. Lett.* **2007**, *91*, No. 012112.

- (46) Nowy, S.; Ren, W.; Elschner, A.; Lövenich, W.; Brütting, W. Impedance Spectroscopy as a Probe for the Degradation of Organic Light-Emitting Diodes. *J. Appl. Phys.* **2010**, *107*, No. 054501.
- (47) Bisquert, J.; Garcia-Belmonte, G.; Pitarch, A.; Bolink, H. J. Negative Capacitance Caused by Electron Injection through Interfacial States in Organic Light-Emitting Diodes. *Chem. Phys. Lett.* **2006**, *422*, 184–191.
- (48) Guan, M.; Niu, L.; Zhang, Y.; Liu, X.; Li, Y.; Zeng, Y. Space Charges and Negative Capacitance Effect in Organic Light-Emitting Diodes by Transient Current Response Analysis. *RSC Adv.* **2017**, *7*, 50598–50602.
- (49) Kim, S. H.; Choi, K.-H.; Lee, H.-M.; Hwang, D.-H.; Do, L.-M.; Chu, H. Y.; Zyung, T. Impedance Spectroscopy of Single- and Double-Layer Polymer Light-Emitting Diode. *J. Appl. Phys.* **2000**, *87*, 882–888.
- (50) Chen, C.-C.; Huang, B.-C.; Lin, M.-S.; Lu, Y.-J.; Cho, T.-Y.; Chang, C.-H.; Tien, K.-C.; Liu, S.-H.; Ke, T.-H.; Wu, C.-C. Impedance Spectroscopy and Equivalent Circuits of Conductively Doped Organic Hole-Transport Materials. *Org. Electron.* **2010**, *11*, 1901–1908.
- (51) Han, S. M.; Kim, K. P.; Choo, D. C.; Kim, T. W.; Seo, J. H.; Kim, Y. K. Equivalent Circuit Models in Organic Light-Emitting Diodes Designed Using a Cole-Cole Plot. *Mol. Cryst. Liq. Cryst.* **2007**, *470*, 279–287.
- (52) Cheon, K. O.; Shinar, J. Electroluminescence Spikes, Turn-off Dynamics, and Charge Traps in Organic Light-Emitting Devices. *Phys. Rev. B* **2004**, *69*, 201306.
- (53) Liu, R.; Gan, Z.; Shinar, R.; Shinar, J. Transient Electroluminescence Spikes in Small Molecular Organic Light-Emitting Diodes. *Phys. Rev. B* **2011**, *83*, 245302.